scientific reports

Check for updates

OPEN

Surface renewal driven copper recovery by cementation in a stirred reactor with a rotating wiper mechanism

A. S. Fathalla[1], E.-S. Z. El-Ashtoukhy[1], M. H. Abdel-Aziz[2]✉, G. H. Sedahmed[1] & M. A. El-Naggar[1,3]

The rate of Cu^{2+} cementation on a Zn cylindrical sheet lining the inner wall of a cylindrical batch-stirred reactor was studied, where a U-shaped wiper consisting of two plastic-coated steel rods was used to agitate the solution. The novelty of the reactor lies in the integration of a rotating U-shaped wiper that provides simultaneous mechanical surface renewal and bulk agitation, enhancing copper removal efficiency without the need for additional stirring mechanisms. Variables studied were wiper rotational speed, wiper diameter, pH of the solution, and the initial concentration of $CuSO_4$ solution. The results revealed that the rate of cementation was unaffected by pH, however, it was increased by increasing other variables. Under optimized operational conditions, the wiper-assisted cementation process achieves nearly complete removal of Cu^{2+} ions from solution within 10 min. Mechanical power consumption measurements indicated that the reactor is energy efficient when the cell is agitated using a large-diameter wiper that rotates at relatively low speeds.

Keywords Copper powder, Diffusion-controlled cementation, Energy efficiency, Heavy metal removal, Rotating wiper, Wastewater treatment

List of symbols

A	Reaction surface area [m^2]
a	Constant [−]
b	Constant [−]
C_o	Concentration at any time, t [mol/m^3]
C	Distance from the open face to the center of the matrix block, m
c	Constant [−]
D	Diffusuivity of Cu^{2+} [m^2/s]
d_{disc}	Disk diameter [m]
d_h	Hole diameter [m]
d_n	Nozzle diameter [m]
d_T	Tank diameter [m]
d_w	Wiper diameter [m]
h	Fixed bed height [m]
k	Mass transfer coefficient [m/s]
l	Distance between jet nozzle and disc [m]
N	Wiper rotational speed [rpm]
Q	Solution volume [m^3]
t	Reaction time [s]
X	Suspended solid particles to liquid ratio [-]

Greek letters

δ	Diffusion layer thickness [m]

[1]Chemical Engineering Department, Faculty of Engineering, Alexandria University, Alexandria 21544, Egypt. [2]Chemical and Materials Engineering Department, King Abdulaziz University, Rabigh 21911, Saudi Arabia. [3]Department of General Subjects, University of Business and Technology, Jeddah 21432, Saudi Arabia. ✉email: mhmousa@alexu.edu.eg

$\in$ Specific power consumption [W/kg]
μ Solution viscosity [kg/m/s]
ρ Solution density [kg/m^3]

Dimensionless groups

J J-factor of mass transfer [$\frac{Sh}{Re\ Sc^{0.33}}$]

Re Reynolds number [$\frac{\rho\ N\ d_w^2}{60\ \mu}$]

Sc Schmidt number [$\frac{\mu}{\rho\ D}$]

Sh herwood number [$\frac{k\ d_T}{D}$]

Copper ions are discharged by the wastewater of many industries, such as printed circuit etching solutions, electroplating rinsing solutions, electropolishing rinsing solutions of copper and its alloys, acid mine drainage solutions, etching and pickling solutions of copper and its alloys, rinsing solutions of electrowinning, and electrorefining of copper. Removal of copper ions from wastewater is of significant environmental interest owing to their potential toxicity to aquatic organisms, besides their ability to impede the biodegradation of organic pollutants present in wastewater[1,2]. Several treatment methods are used to remove copper ions from waste solutions, such as chemical precipitation[3,4], electrocoagulation[5,6], adsorption[7], ion exchange[8,9], bioremediation[10,11], and reverse osmosis[12].

Among the various available techniques, one particularly attractive method is cementation, a well-established metallurgical process that offers operational simplicity and cost-effectiveness[1,13]. Cementation is a redox-based metal recovery process wherein dissolved metal ions, such as Cu^{2+}, are reduced and deposited as solid metal onto the surface of a more reactive (less noble) metal, such as zinc, which simultaneously dissolves into the solution.

According to the electrochemical theory[14,15], cementation of copper ions on Zn surfaces takes place throughout the formation of a multitude of microscopic galvanic cells of the type $Zn|Zn^{2+}Cu^{2+}|Cu$, where the overall reaction governing the process is:

$$Zn + Cu^{2+} \rightarrow Zn^{2+} + Cu \tag{1}$$

Cementation of Cu^{2+} on Zn is also used in the electrowinning of Zn to purify the leach $ZnSO_4$ solution from Cu^{2+} impurity, which is left without removal and contaminates the cathodically deposited Zn and reduces its current efficiency.

Previous studies[16–20] reported that the above reaction is diffusion-controlled, where the diffusion of Cu^{2+} from the solution bulk to the Zn surface is the rate-determining step. Hence, augmenting the rate of cementation may result from enhancing the rate of mass transfer of copper ions through the diffusion boundary layer established at the zinc surface. Table 1 summarizes some relevant studies carried out to intensify the rate of Cu^{2+} cementation by different means of increasing the relative solution velocity between the solution and the Zn surface.

During the cementation process, a porous copper powder layer is continuously built on the Zn surface. Increasing the thickness of this deposited layer inhibits further diffusion of copper ions from the bulk solution and consequently decreases the rate of cementation[29,30]. Intensifying the rate of cementation by scrapping the cementing surface regularly may contribute to removing the porous layer of copper powder from the Zn surface by which the rate of cementation increases, besides, the reacting surface solution is renewed by dragging away the reacted solution and replacing it with a fresh supply of the bulk solution (surface renewal).

Authors [ref.]	Zinc surface geometry	Overall mass transfer correlation
El-Shazly et al. [21]	Perforated reciprocating disc	$\boldsymbol{Sh} = 89\ \boldsymbol{Re}^{0.537}\ \boldsymbol{Sc}^{0.33}\left(\frac{\boldsymbol{d}}{\boldsymbol{d_h}}\right)^{-0.496}$
Mubarak[20]	A cylindrical sheet lining the wall of an agitated vessel fitted with four traditional baffles	$\boldsymbol{Sh} = 0.035\ \boldsymbol{Re}^{0.89}\ \boldsymbol{Sc}^{0.33}$
Nosier et al.[22]	Solid rod (in the presence of suspended ceramics particles) in a batch recirculating reactor	$\boldsymbol{J} = 2.76\ \boldsymbol{Re}^{-0.5211}\ \boldsymbol{X}^{0.5233}$
Konsowa[23]	Horizontal disc impinged by an axially-flow submerged jet	$\boldsymbol{Sh} = 0.306\ \boldsymbol{Re}^{0.997}\ \boldsymbol{Sc}^{0.33}\ (\boldsymbol{d_n}/\boldsymbol{l})^{0.0337}$
Amin and El-Ashtoukhy[24]	Raschig rings in a rotating packed bed	$\boldsymbol{Sh} = 0.0005\ \boldsymbol{Re}^{0.947}\ \boldsymbol{Sc}^{0.33}$
El-Sayed et al.[25]	A longitudinal finned rotating cylinder	$\boldsymbol{Sh} = 0.74\ \boldsymbol{Re}^{0.69}\ \boldsymbol{Sc}^{0.33}$
El-Shazly et al.[26]	Fixed bed of cylinders placed in a recirculating batch reactor	With a calming section: $\boldsymbol{Sh} = 2.1\ \boldsymbol{Re}^{0.867}\ \boldsymbol{Sc}^{0.33}\ (\boldsymbol{d}/\boldsymbol{h})^{-1.02}$ Without a calming section: $\boldsymbol{Sh} = 2.3\ \boldsymbol{Re}^{0.87}\ \boldsymbol{Sc}^{0.33}\ (\boldsymbol{d}/\boldsymbol{h})^{-0.96}$
Ibrahim et al.[27]	A cylindrical sheet lining the wall of an agitated vessel provided with extended perforated baffles	Axial flow impeller: $\boldsymbol{Sh} = 0.044\ \boldsymbol{Re}^{0.87}\ \boldsymbol{Sc}^{0.33}$ Radial flow impeller: $\boldsymbol{Sh} = 0.045\ \boldsymbol{Re}^{0.91}\ \boldsymbol{Sc}^{0.33}$
Elzahaby et al.[28]	Horizontal disc impinged by an axially- turbulent flow unsubmerged jet	$\boldsymbol{Sh} = 0.19\ \boldsymbol{Re}^{0.9}\ \boldsymbol{Sc}^{0.33}\ (\boldsymbol{l}/\boldsymbol{d_{disc}})^{-0.68}$

Table 1. Previous relevant studies on the cementation of copper on Zn surfaces of different geometries.

Despite the clear benefit of enhancing mass transfer by wiping the cementing surface, this approach has not been widely investigated in cementation systems, particularly those involving zinc-lined cylindrical reactors. Ahmed et al.[31] explored the effect of inserting a stationary wiper almost touching a rotating Zn solid cylinder on the rate of copper ions cementation. Compared to a smooth revolving cylinder with no wiper, the authors reported that the wiper enhanced the rate of cementation by an amount ranging from 8.9 to 170.6%, depending on the rotational speed. Farooque and Fahidy[32] and Takahashi et al.[33] used a stationary wiper blade to enhance the rate of mass transfer at a rotating cylinder electrode in processes such as anodic oxidation of methanol and electrolytic recovery of metals, respectively.

The present study aims to investigate the rate of copper ion (Cu^{2+}) removal from wastewater through the cementation process, using a zinc cylindrical sheet that lines the inner wall of a stirred cylindrical tank reactor. The study explores the use of a rotating wiper mechanism that simultaneously agitates the solution and renews the zinc surface, thereby enhancing the rate of copper cementation. This configuration, which employs a U-shaped rotating wiper made of plastic-coated steel rods to both agitate the solution and periodically remove accumulated copper deposits from the zinc surface, has not been previously reported. The design is intended to improve mass transfer and sustain high reaction efficiency. The study also seeks to determine the operating conditions that optimize copper removal while minimizing energy consumption. In parallel, the energy consumed by the wiper's rotation was measured to assess the reactor's energy utilization efficiency, to identify operation conditions that achieve effective copper removal with minimal power requirements.

The novelty of the present reactor lies in its reversed configuration compared to previously reported systems, such as the one proposed by Ahmed et al.[31], where a stationary wiper was used against a rotating solid zinc cylinder. In the current design, a U-shaped rotating wiper agitates the bulk $CuSO_4$ solution while simultaneously wiping a fixed zinc sheet lining the reactor wall. This approach offers several advantages: (i) a significantly larger reactive surface area, (ii) more uniform and continuous surface renewal, and (iii) enhanced turbulence due to boundary layer separation and eddy formation in the wake of the rotating rods. Unlike the single-point wiping in previous designs, the present configuration integrates mass transfer enhancement and energy efficiency in a single, mechanically simple setup.

Experimental part

Apparatus

A real image of the set-up used in the present study is presented in Fig. 1A, while the full-detailed setup is shown in Fig. 1B. It consisted of a 15 cm diameter and 20 cm height cylindrical plexiglass container lined internally with a Zn cylindrical sheet. The backside of the Zn sheet was coated with epoxy resin to prevent exposure to the solution, thereby avoiding unwanted cementation or corrosion on the rear surface and ensuring that only the inner surface contributed to the reaction. A rotating U-shaped wiper made of plastic-coated steel rods was used

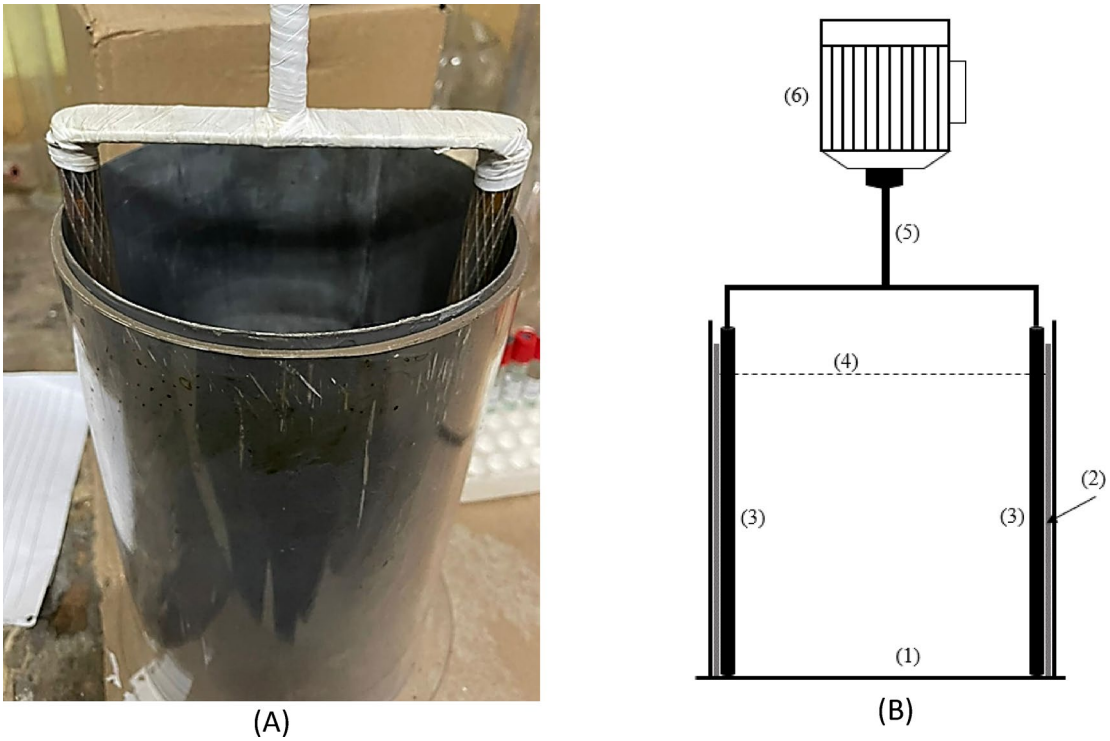

Fig. 1. Experimental set-up. (**A**) Real image, (**B**) Schematic diagram; (1) Plexiglass container, (2) Zn sheet lining the inner wall of the container, (3) Plastic-coated steel rods (rotating wiper), (4) Solution level, (5) epoxy-resin insulated steel shaft, (6) Variable-speed motor.

Variable	Typical range
Wiper rotational speed	100, 140, 180, 220, 260, and 300
Wiper diameter (cm)	0.8, 1.1, and 1.4
pH	2, 3, 4, and 5
Initial concentration of $CuSO_4$ solution (mol/L)	0.025, 0.075, and 0.125

Table 2. Variables studied in the present work and their typical ranges.

$CuSO_4$ conc. (mol/L)	ρ (g/cm^3)	$\mu \times 10^2$ (g/cm.s)	$D \times 10^6$ (cm^2/s)	Schmidt number (Sc)
0.025	1.003	1.1	6.37	1722
0.075	1.012	1.12	6.075	1822
0.125	1.02	1.15	5.73	1968

Table 3. Physical properties of copper sulfate solutions measured at 25 ± 2℃.

to agitate the $CuSO_4$ solution placed in the vessel, where the wiper was connected to a variable-speed digital motor through an insulated steel shaft. The wiper was fixed so that it just touched the zinc cylinder the presence of air gaps between them. All variables studied in the present work are shown in Table 2.

Procedure

Before each run, the zinc cylinder was washed with a 10% HCl solution to remove any oxide film formed on its surface, rinsed with distilled water, and finally dried. Then, two liters of fresh $CuSO_4$ solution were prepared using A.R. grade chemicals, and distilled water was added to the container. The density ($\boldsymbol{\rho}$) and viscosity ($\boldsymbol{\mu}$) of all solutions used were determined using a density bottle and an Ostwald viscometer, respectively[34], while the diffusivity of copper ions ($\boldsymbol{D}$) was obtained from the literature[35] at the experimental temperature of 25ºC. Table 3 shows the physical properties of copper sulfate solutions measured at $25 \pm 2^{\circ}C$. This temperature range was selected as it reflects typical ambient laboratory conditions and avoids the complexity of external temperature control. A deviation of ± 2 °C has a negligible influence on the measured physical properties and does not significantly impact the accuracy of mass transfer coefficient estimations.

The reaction kinetics were studied during the run by withdrawing a 5 mL solution sample at a constant time interval for Cu^{2+} analysis. The % removal of copper ions was determined by the equation:

$$\%removal = \left(\frac{C_o - C}{C_o}\right) \times 100 \tag{2}$$

where C_o and C are the solution concentrations at the beginning and at time t, respectively. The energy consumed by the rotating wiper was measured by a Wattmeter as mentioned elsewhere[36].

The Cu^{2+} concentrations were determined using a DR 3900 HACH UV–Vis spectrophotometer at 810 nm, with a photometric accuracy of ± 0.005 Abs and wavelength accuracy of ± 1 nm. Each measurement was repeated three times, and the average was recorded. The standard deviation among replicates was below 2%, indicating good precision. Calibration curves prepared using standard Cu^{2+} solutions yielded R^2 values > 0.999, and blank corrections were performed for all samples to ensure accuracy.

Results and discussions

Determination of the mass transfer coefficient

Since cementation of copper ions on zinc is a mass transfer-limited reaction, the effect of the variables studied in the present work (Table 2) on the rate of copper ions cementation can be expressed in terms of the mass transfer coefficient ($\boldsymbol{k}$) which can be calculated for the present batch reactor by the following Eqs.[37,38]:

$$-Q\frac{dC}{dt} = kAC \tag{3}$$

which, upon integration, gives:

$$\ln\left(\frac{C_o}{C}\right) = \frac{k\,A}{Q}\,t \tag{4}$$

where A is the active area of the Zn cylinder and Q is the volume of the solution. The mass transfer coefficient was determined from the slope $\left(\frac{k\,A}{Q}\right)$ of the straight-line plot of $\ln\left(\frac{C_o}{C}\right)$ versus t as shown in Fig. 2.

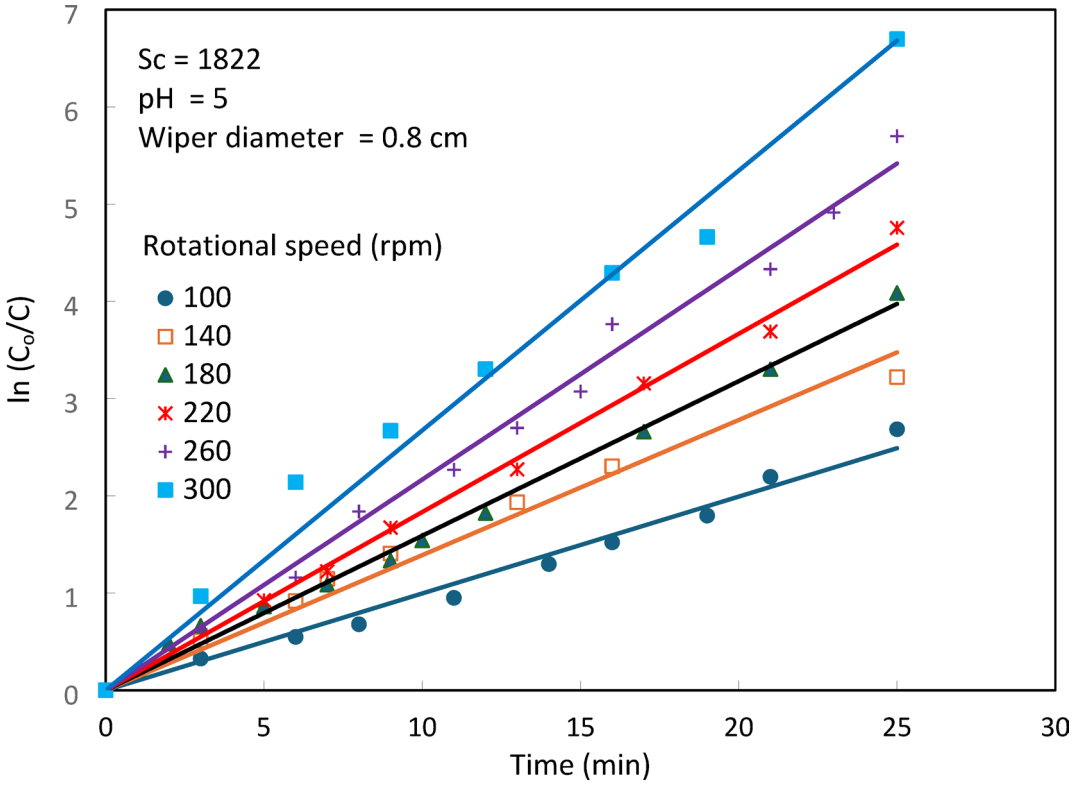

Fig. 2. Typical $\ln\left(\frac{C_o}{C}\right)$ Versus t.

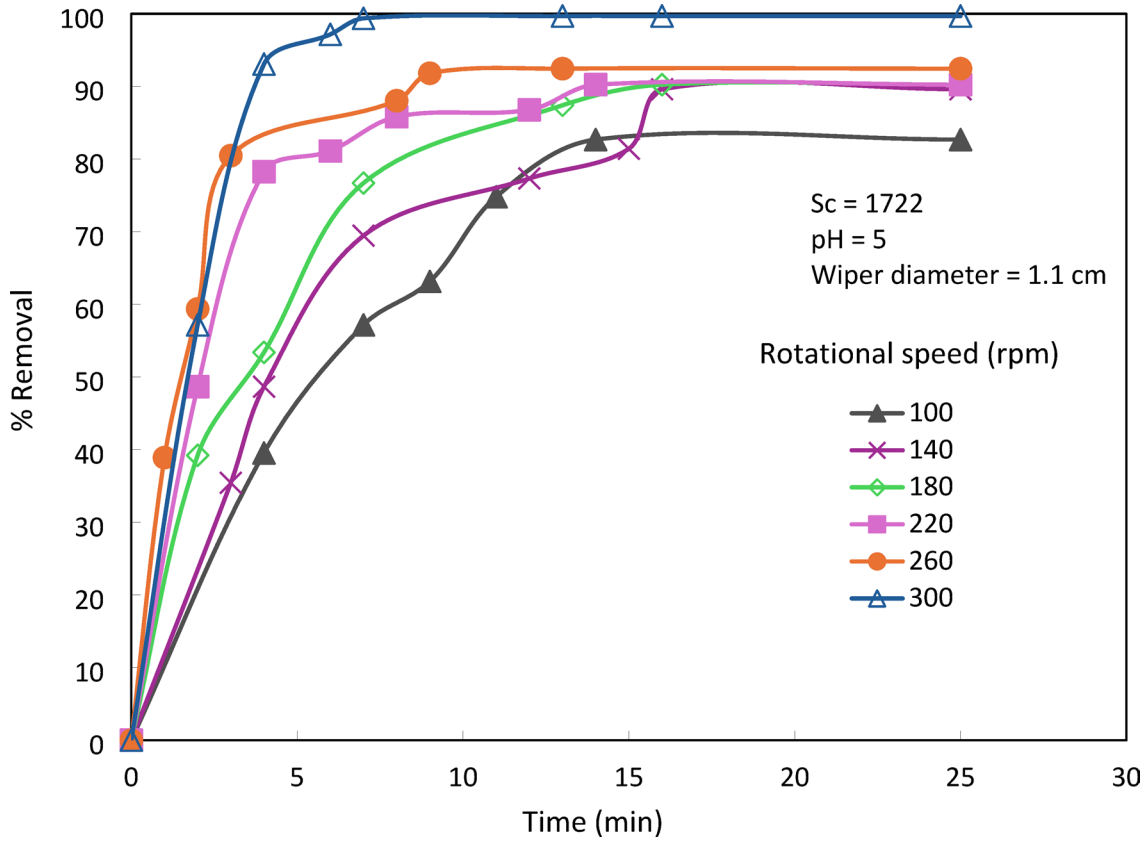

Fig. 3. Effect of wiper rotational speed on the rate of Cu^{2+} cementation.

Effect of wiper rotational speed

Figure 3 shows that the % removal of Cu^{2+} increases with increasing wiper rotational speed. This may be ascribed to the following effects:

As the wiper touches the Zn wall at a certain location, it removes the reacted solution from the wall, then the solution is replenished with a fresh solution from the bulk with a subsequent increase in the rate of mass transfer according to Eq. (3) (surface renewal mechanism[39]). This surface renewal occurs periodically as the rotating wiper sweeps across the Zn surface, displacing the depleted boundary layer and replacing it with fresh bulk solution. The frequency of this renewal is directly related to the wiper's rotational speed (rpm), meaning each revolution introduces a new contact point and a corresponding renewal event. In addition, the motion of the wiper induces turbulence in its wake, promoting further convective mixing and boundary layer thinning between wiper passes. As a result, although the renewal is periodic, the combination of mechanical contact and hydrodynamic effects provides a quasi-continuous enhancement of mass transfer.

Reduction in the thickness of both the hydrodynamic and the underlying diffusion boundary layers established at the zinc cylinder as a result of the increase in the degree of turbulence generated in the wake of the rotating cylindrical wiper as a result of boundary layer separation[39]. The reduction in the diffusion boundary layer thickness (δ) increases the mass transfer coefficient at the zinc cylinder as given by the equation[38]:

$$k = \frac{D}{\delta} \tag{5}$$

Effect of initial $CuSO_4$ concentration

Figure 4 shows that the rate of copper ions cementation (represented by the % removal) increases by increasing the initial concentration of $CuSO_4$ (i.e., Schmidt number) owing to the following effects:

(i) By increasing the initial concentration of $CuSO_4$, the driving force of the diffusion-limited cementation reaction increases, resulting in a higher mass transfer rate[21,40].

(ii) At higher initial $CuSO_4$ concentrations, the deposited copper is expected to form more irregular and granular layers, as suggested by previous studies on diffusion-controlled cementation processes[41,42]. These morphological features may act as turbulence promoters and enhance local mixing at the solid-liquid interface. While no direct measurements or imaging of the zinc surface were performed in this study, the observed increase in cementation rate is consistent with such surface effects.

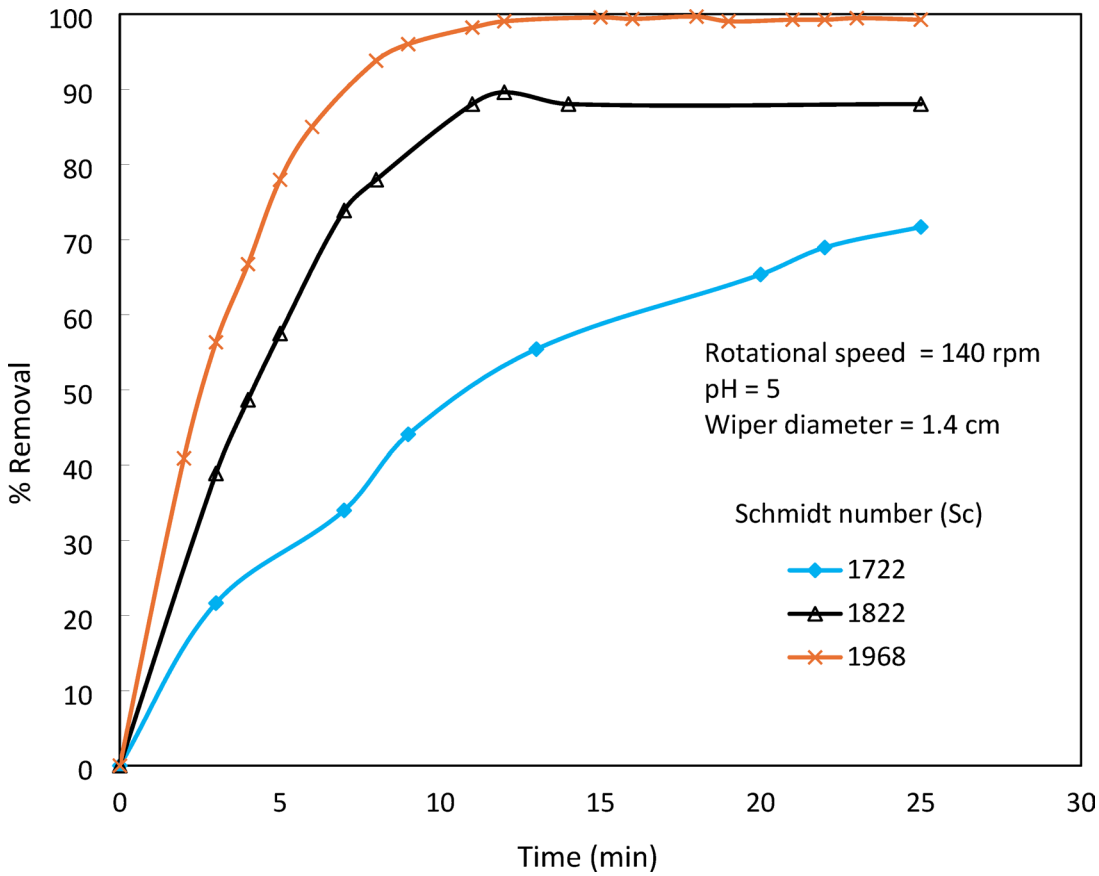

Fig. 4. Effect of initial concentration on the rate of Cu^{2+} cementation.

Figure 4 shows that for a given set of conditions, the higher the value of Sc the higher the rate of mass transfer and the rate of cementation, which is consistent with the hydrodynamic boundary layer theory[43].

Effect of wiper diameter

To explain the effect of wiper diameter on the rate of cementation, some light should be shed on the enhancement mechanism during wiper rotation. Previous studies on using stationary wipers on rotating surfaces have revealed that wiping enhances the rate of heat or mass transfer via a surface renewal mechanism where fresh solution rushes to the wiped location to replace the depleted solution removed by the wiper. In the present case where the cylindrical wiper is rotating in the solution, an extra effect comes into the picture where turbulent eddies are generated in the wake of the moving cylindrical wiper due to the separation of the boundary layer surrounding the wiper[39]. These generated eddies contribute to enhancing the rate of mass transfer at the Zn wall by thinning the diffusion layer (Eq. 5).

Figure 5. depicts that increasing the diameter of the rotating wiper increases the rate of cementation. As the wiper diameter increases, the Reynolds number of the wiper increases along with the intensity of the induced eddies, with a subsequent increase in the wall rate of cementation. Also, as the wiper diameter increases, the area swept by the wiper increases with a subsequent increase in the amount of solution that rushes to the wiped location to renew the surface with a fresh supply of reactant.

It should be noted that while increasing the wiper diameter enhances the intensity of turbulence and surface renewal within the tested range, further increases beyond this range may produce adverse hydrodynamic effects. Specifically, oversized wipers can generate broad boundary layer separation zones and unstable eddy structures, leading to flow detachment, dead zones, and a reduction in the effective shear stress at the zinc surface. These effects may lead to a thickened boundary layer and reduced mass transfer efficiency.

Although direct imaging of the Zn surface before and after wiping (e.g., via SEM or optical microscopy) was not performed, the effectiveness of the mechanical wiping action was indirectly confirmed by the consistent enhancement in Cu^{2+} removal efficiency and mass transfer coefficient with increasing wiper diameter and rotational speed. These trends indicate that the rotating wiper maintained effective and continuous contact with the Zn surface, successfully removing deposited copper and renewing the diffusion layer. This validates the functionality of the surface renewal mechanism and highlights the effectiveness of the reactor design. While the force exerted by the wiper was not directly measured or simulated, future studies may incorporate mechanical analysis or modeling to further optimize the wiper–surface interaction and enhance design performance.

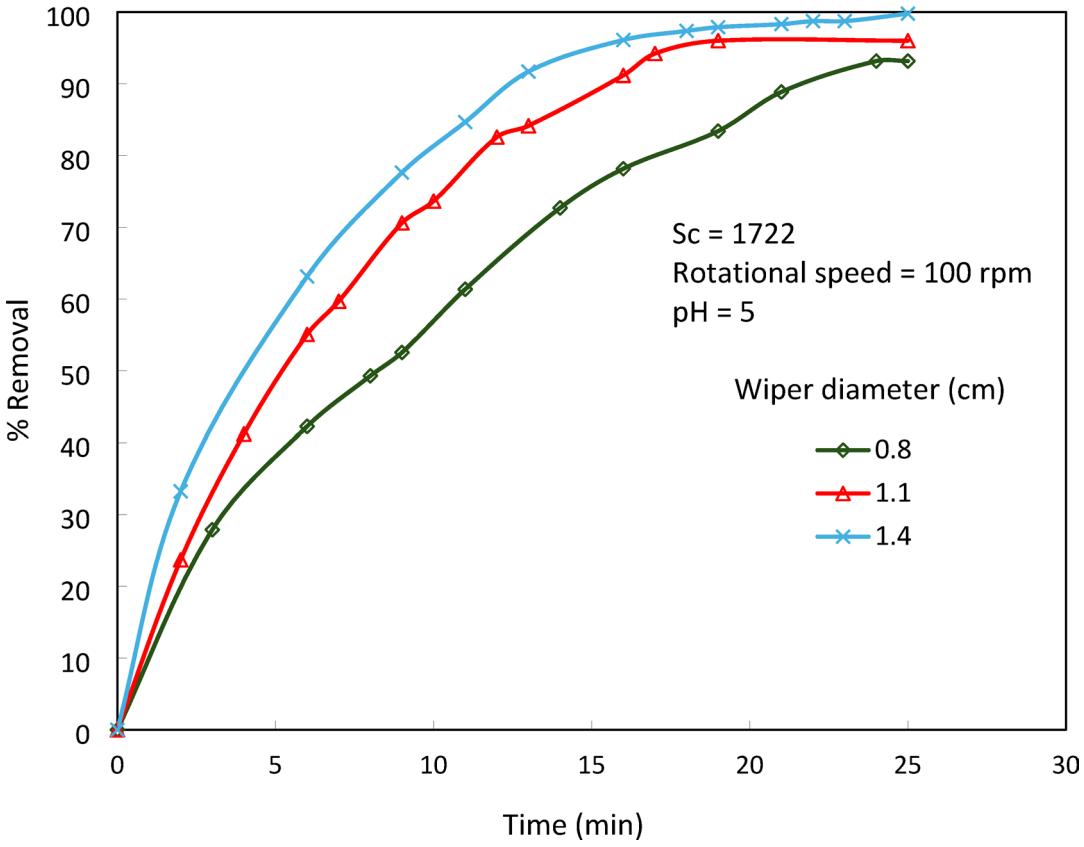

Fig. 5. Effect of wiper diameter on the rate of Cu^{2+} cementation.

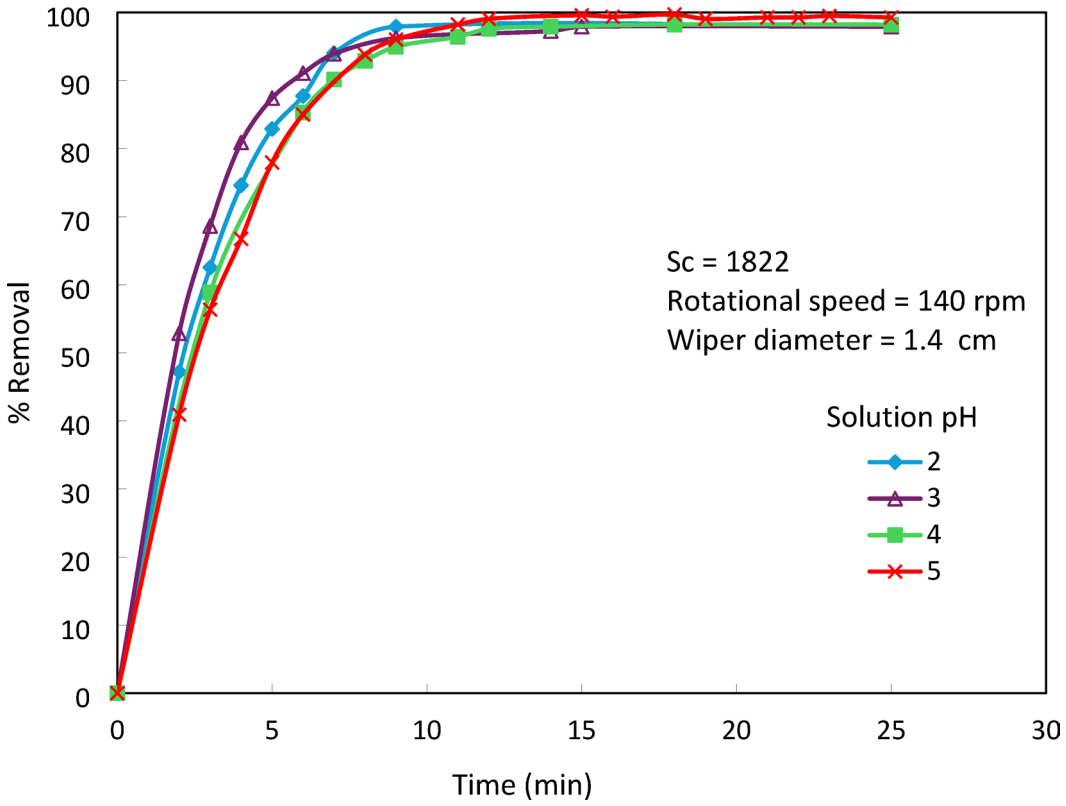

Fig. 6. Effect of initial solution pH on the rate of Cu^{2+} cementation.

Effect of solution pH

Figure 6 shows that within the pH range 2–5, the pH of the solution has a negligible effect on the rate of copper cementation, even at low pH values such as 2 and 3, where H_2 is likely to evolve simultaneously with copper deposition according to the reaction:

$$\boldsymbol{Zn} + 2\boldsymbol{H}^{+} \rightarrow \boldsymbol{Zn}^{2+} + \boldsymbol{H}_2 \tag{6}$$

The fact that there is little difference between the effects of low and high pH values on the rate of copper cementation suggests that the simultaneous H_2 evolution on Zn according to the above reaction is sluggish because of the high H_2 overpotential on Zn[37]. In other words, the slow rate of H_2 evolution on Zn is thermodynamically attributed to the high activation energy of the above reaction[37], i.e., Zn acts as a negative catalyst for H_2 evolution.

Mass transfer data correlation

To assist in scaling up, designing, and operating industrial reactors, the rate of cementation indicated by the mass transfer coefficient was included in an empirical dimensionless correlation of the form:

$$Sh = a\, Re^{b} Sc^{0.33} \left(\frac{d_W}{d_T}\right)^{c} \tag{7}$$

where a, b, and c are constants.

In calculating the Reynolds number (Re) and Sherwood number (Sh), the wiper diameter (d_w) and the tank diameter (d_T) were taken as the characteristic lengths, respectively. The exponent of the Schmidt number (Sc) was fixed at the value 0.33 according to previous mass transfer studies about the removal of heavy metals from waste solutions by cementation[29,37]. A sensitivity analysis was also performed by varying the Schmidt number exponent between 0.2 and 0.5 to assess its effect on the model's accuracy. The analysis showed that the value 0.33 resulted in the lowest average deviation and best correlation with experimental data, confirming the appropriateness of this choice for the present system.

Figures 7 and 8, and 9 show that for the conditions $1722 < \boldsymbol{Sc} < 1968$, $95 < \boldsymbol{Re} < 895$, $\boldsymbol{pH} = 5$, and $0.053 < \left(\frac{d_W}{d_T}\right) < 0.093$, the present mass transfer data fit the equation:

$$Sh = 6.2\, Re^{0.7} Sc^{0.33} \left(\frac{d_W}{d_T}\right)^{-0.67} \tag{8}$$

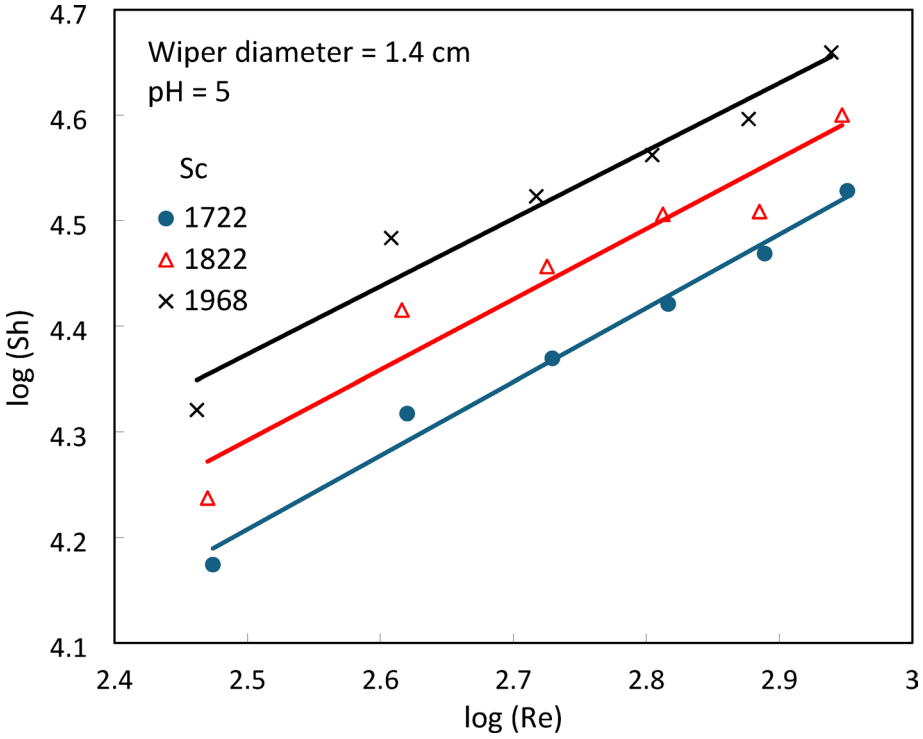

Fig. 7. log Sh versus log Re.

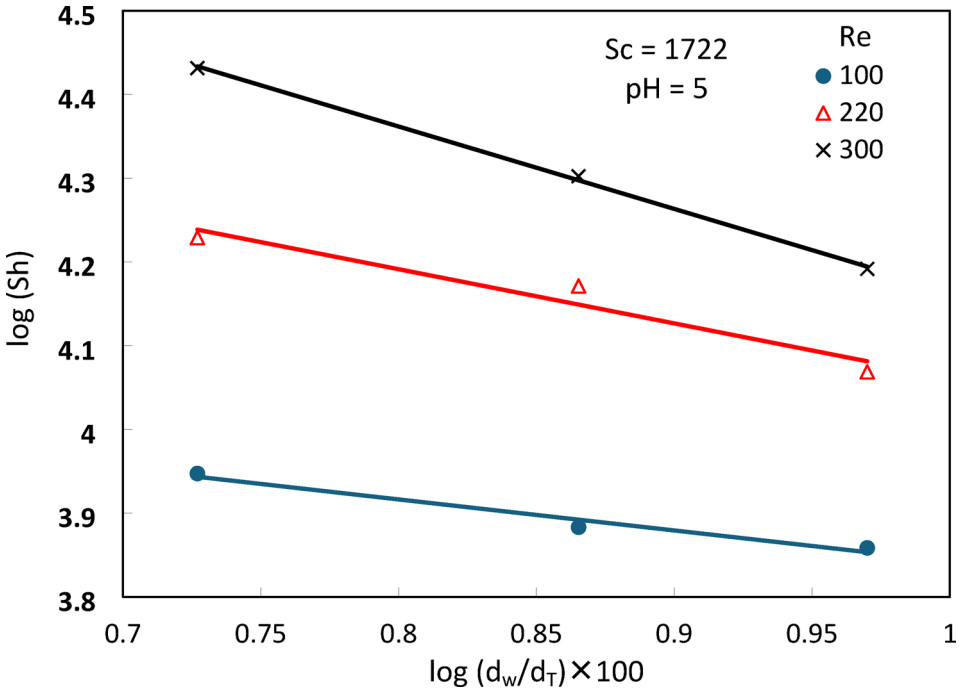

Fig. 8. Log Sh versus log (d_w/d_T).

with an average deviation of $\pm$ 9.5%.

The specific form of the dimensionless correlation in Eq. (8) was selected to reflect the distinct hydrodynamic behavior introduced by the rotating wiper mechanism. While many classical correlations for agitated systems follow the general form $Sh \propto Re^b\ Sc^{0.33}$, the inclusion of the geometric ratio (d_w/d_T) in the model accounts for the localized mixing effects caused by the wiper's motion relative to the reactor size. The elevated Reynolds number exponent (0.7), higher than in many conventional systems, suggests that mass transfer in this setup is

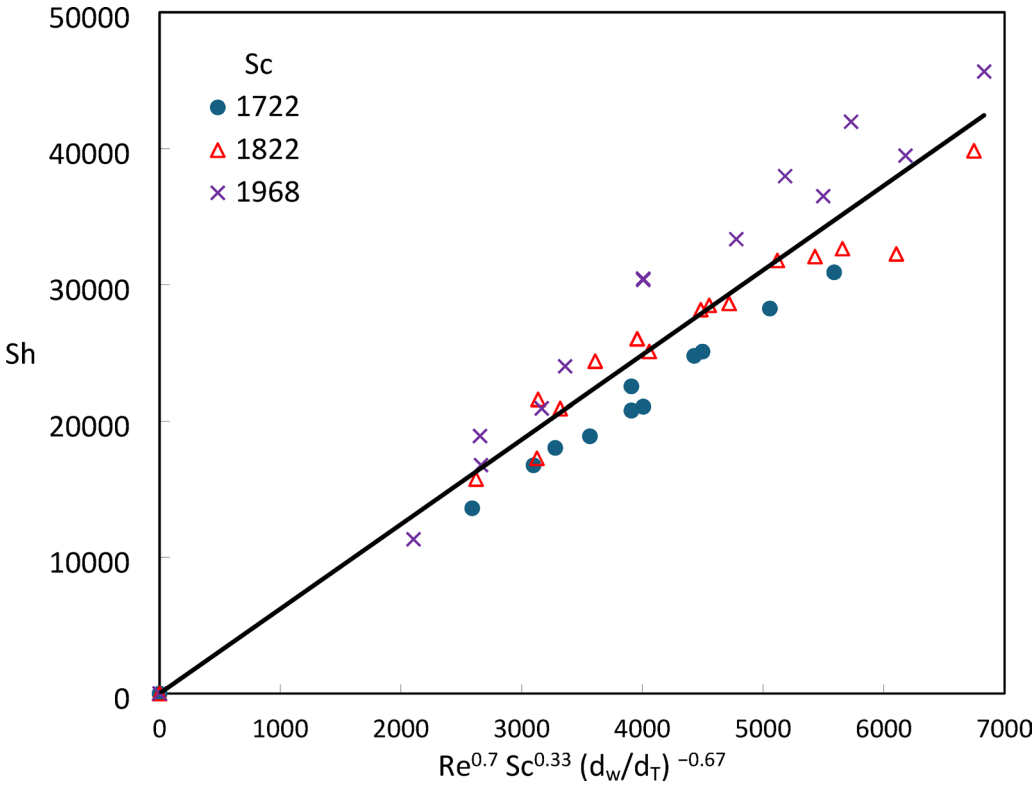

Fig. 9. Overall mass transfer correlation for the present data.

strongly influenced by wiper-induced turbulence and periodic boundary layer disruption. This distinguishes the present correlation from traditional impeller-based models and supports its suitability for capturing the unique transport dynamics of the current reactor configuration.

The high value of the (6.2) constant indicates that the deposited copper layer on the zinc cylinder is rough and non-uniform[31,44]. Equation (8) shows that the dependence of the mass transfer coefficient (k) on the rotational speed (N) and the wiper diameter (d_w) is given by:

$$k \propto N^{0.7} \tag{9}$$

$$k \propto d_w^{0.73} \tag{10}$$

The above equations show that the wiper diameter had a more powerful effect on the rate of cementation than the rotational speed. Previous studies on the enhancement of heat and mass transfer by wiping[45,46] have concluded that mass and heat transfer take place during wiping by a surface renewal mechanism, which leads to the following proportionality:

$$Sh \propto Re^{0.5} \tag{11}$$

The discrepancy between the exponent 0.5 and the present exponent 0.7 may be attributed to the fact that in the present case, the rate of diffusion-controlled cementation is enhanced not only due to the surface renewal mechanism but also owing to hydrodynamic boundary layer separation where eddies are formed in the wake of the wiper in the vicinity of the Zn surface. It seems that the contribution of the effect of eddy formation in the wake of the wiper is responsible for the high Re exponent 0.7.

Although real-scale industrial validation was not possible within the scope of this study, the proposed mass transfer correlation was subjected to alternative validation steps to ensure its applicability for scale-up. These included checking the dimensional consistency and conformity with classical mass transfer analogies involving the Sherwood, Reynolds, and Schmidt numbers. Furthermore, the experimental results were reproducible across independent trials, and the obtained exponents are consistent with those reported in similar studies involving diffusion-controlled cementation systems. These considerations support the reliability of the correlation for use in preliminary scale-up and reactor design, particularly in systems operating under similar hydrodynamic and geometric conditions.

Energy utilization efficiency

Since increasing the rotational speed of the wiper enhances the volumetric mass transfer coefficient (kA) which refers to the productivity of the reactor, the energy consumed in rotating the wiper increases, too. Hence, the

N (rpm)	d_w = 1.4 cm			d_w = 1.1 cm			d_w = 0.8 cm		
	kA (cm³/s)	$\in$ (W/kg)	$\frac{kA}{\in}$	kA (cm³/s)	$\in$ (W/kg)	$\frac{kA}{\in}$	kA (cm³/s)	$\in$ (W/kg)	$\frac{kA}{\in}$
100	3.38	0.75	4.51	3.08	0.74	4.16	1.56	0.75	2.1
140	4.7	1.05	4.48	4.08	1.05	3.9	2.49	1.04	2.39
180	5.3	1.9	2.79	5.1	1.94	2.63	3.8	1.9	2
220	5.97	2.1	2.84	5.68	2	2.84	4.28	2.1	2.03
260	6.67	2.75	2.43	6.4	2.6	2.46	4.77	2.6	1.83
300	7.65	3.45	2.22	7	3.5	2	5.6	3.5	1.6

Table 4. The criterion ($kA/\in$) for several wiper diameters and rotational speeds (Sc = 1722).

best criterion used to evaluate the economic feasibility of the present reactor is the ratio between the volumetric mass transfer coefficient and the specific power consumption of the rotating wiper ($\in$). The specific power consumption was calculated by the equation:

$$\in = \frac{\text{Power consumed in rotating the wiper (Watt)}}{\text{mass of solution (kg)}} \tag{12}$$

where the absolute power consumption was measured using a wattmeter as recommended by different authors who carried out experimental mass transfer studies in agitated vessels[36].

Table 4 shows the variation of criterion (kA/$\in$) with the rotational speed and the diameter of the wiper. The table shows that increasing the rotational speed of the wiper increases the power consumption at higher degrees than the volumetric mass transfer coefficient; thus, the reactor is economically feasible when it operates at a relatively low rotational speed. The table also shows that the power consumption is unaffected by the wiper diameter. Therefore, the mechanical energy utilization efficiency of the present reactor was enhanced by utilizing large-sized wipers that rotate at relatively low speeds.

A preliminary assessment of scale-up feasibility was conducted using the current performance data. Under optimal operating conditions (wiper diameter 1.4 cm, 100 rpm), the system achieved nearly complete removal of Cu^{2+} in 10 min with a specific power consumption of 0.75 W/kg. For a 2-liter batch, this corresponds to an energy requirement of approximately 0.125 kWh/m³ treated. Assuming an initial Cu^{2+} concentration of 0.025 mol/L and complete recovery, this translates to an energy cost of roughly 0.079 kWh/kg of copper removed. These values suggest that the present reactor design is highly energy-efficient and has promising economic potential for scale-up. Future work will include more detailed cost-benefit analyses and system integration studies.

Despite the promising performance of the present reactor design, a few practical limitations should be considered for long-term or industrial-scale implementation. Continuous exposure of the Zn surface to acidic or metal-rich solutions may lead to surface passivation or uneven corrosion, which could affect reaction kinetics and surface renewal over extended periods. Additionally, the accumulation of copper powder in the reaction zone may lead to clogging or resistance to flow between the wiper and the Zn surface, potentially requiring periodic cleaning or filter integration. Finally, while the deposited copper can be recovered in a relatively pure form, its safe disposal or reuse should be addressed as part of a broader resource recovery or environmental management strategy. Future work should investigate these operational challenges in longer-duration trials to evaluate reactor durability and lifecycle performance.

The long-term durability of the Zn liner under repetitive wiping is another consideration for future scale-up. In the present study, the U-shaped wiper was designed to apply only mild mechanical contact, and no visible wear or deterioration of the Zn surface was observed during repeated short-term experimental runs. The use of plastic-coated rods minimized abrasion, and the wiping action was primarily aimed at removing soft copper deposits. However, in extended use, gradual material loss or passivation of the Zn surface may occur due to both chemical and mechanical effects. Assessing the reactor's lifespan under continuous or industrial-scale operation will be an important area for future work.

From an environmental standpoint, the proposed cementation process presents notable sustainability advantages. The use of zinc as a sacrificial agent leads to the formation of zinc sulfate ($ZnSO_4$), which remains dissolved in the treated solution. Importantly, $ZnSO_4$ is widely used in hydrometallurgical processes, particularly as the primary electrolyte in zinc electrowinning and impurity removal stages during zinc refining. This creates a potential for the Zn-containing effluent to be recycled into upstream metallurgical operations, enhancing circularity and reducing waste. Additionally, the process requires no chemical reagents or pH adjustment, generates no sludge, and enables recovery of copper in a reusable solid form, reinforcing its environmental compatibility and industrial relevance.

Conclusions

The present study introduced a novel cylindrical stirred reactor lined with a zinc sheet and equipped with a U-shaped rotating wiper that simultaneously agitates the solution and scrapes the Zn surface during the cementation of Cu^{2+} ions. The effects of key operating variables: wiper diameter, rotational speed, and initial $CuSO_4$ concentration on the rate of cementation were systematically investigated. Results demonstrated that increasing both the wiper diameter and rotational speed significantly enhanced the rate of Cu^{2+} removal, attributed to intensified turbulence, eddy formation, and more frequent surface renewal events. Similarly, higher

$CuSO_4$ concentrations increased the diffusion driving force, further accelerating the process. In contrast, solution pH had a negligible impact within the tested range, confirming the diffusion-controlled nature of the reaction.

The experimental data were used to derive an empirical mass transfer correlation using dimensional analysis, which captures the combined influence of flow dynamics and physical properties on the mass transfer coefficient. The high exponent of the Reynolds number (0.7) suggests that, in addition to the classical surface renewal mechanism, strong boundary layer separation and turbulent eddy formation significantly enhance mass transfer.

From an energy efficiency perspective, the reactor showed optimal performance when operated with a large-diameter wiper (1.4 cm) at relatively low speeds (100–140 rpm), achieving nearly complete Cu^{2+} removal within 10 min while maintaining low specific power consumption.

Compared to previous cementation systems, this work is distinguished by the introduction of a rotating wiper mechanism that provides simultaneous surface agitation and renewal, enabling high removal efficiency with minimal energy input. The integration of mechanical wiping with stirring represents a practical advancement in the design of energy-efficient reactors for heavy metal recovery from wastewater. This reactor design and its associated correlation offer a valuable basis for future scale-up and industrial implementation.

While the present study focused on optimizing reactor geometry, hydrodynamic parameters, and energy efficiency, future work may include a detailed analysis of the recovered copper powder using techniques such as XRD or ICP-OES to assess its purity and support its potential reuse, thereby enhancing the sustainability profile of the proposed system.

Data availability

The datasets used and/or analysed during the current study available from the corresponding author on reasonable request.

Received: 17 May 2025; Accepted: 7 July 2025
Published online: 10 August 2025

References

1. Al-Saydeh, S. A., El-Naas, M. H. & Zaidi, S. J. Copper removal from industrial wastewater: A comprehensive review. *J. Ind. Eng. Chem.* **56**, 35–44 (2017).
2. Vardhan, K. H., Kumar, P. S. & Panda, R. C. A review on heavy metal pollution, toxicity and remedial measures: current trends and future perspectives. *J. Mol. Liq.* **290**, 111197 (2019).
3. Pohl, A. Removal of heavy metal ions from water and wastewaters by sulfur-containing precipitation agents. *Water Air Soil. Pollut.* **231**, 503 (2020).
4. Benalia, M. C., Youcef, L., Bouaziz, M. G. & Achour, S. Menasra, removal of heavy metals from industrial wastewater by chemical precipitation: mechanisms and sludge characterization. *Arab. J. Sci. Eng.* **47**, 5587–5599 (2022).
5. Kilany, A. Y., Abdel-Aziz, M. H., Nosier, S. A., Hussein, M. & Sedahmed, G. H. Electrocoagulation for the treatment of metals machining plants effluents: experimental and modeling study. *Chem. Eng. Technol.* **46**, 1521–1532 (2023).
6. Kamaraj, R., Ganesan, P., Lakshmi, J. & Vasudevan, S. Removal of copper from water by electrocoagulation process–effect of alternating current (AC) and direct current (DC). *Environ. Sci. Pollut Res.* **20**, 399–412 (2013).
7. El-Shafey, E. S. I. & Al-Kindy, S. M. Z. Removal of Cu^{2+} and $Ag^{+}$from aqueous solution on a chemically-carbonized sorbent from date palm leaflets. *Environ. Technol.* **34**, 395–406 (2013).
8. Abel-Aziz, M. H., Nirdosh, I. & Sedahmed, G. H. Ion-exchange-assisted electrochemical removal of heavy metals from dilute solutions in a stirred-tank electrochemical reactor: A mass-transfer study. *Ind. Eng. Chem. Res.* **52**, 11655–11662 (2013).
9. Siu, P. C. C., Koong, L. F., Saleem, J., Barford, J. & McKay, G. Equilibrium and kinetics of copper ions removal from wastewater by ion exchange. *Chin. J. Chem. Eng.* **24**, 94–100 (2016).
10. Rehan, M. & Alsohim, A. S. Bioremediation of Heavy Metals, in *Environmental Chemistry and Recent Pollution Control Approaches* (Eds.) H. S.-Norena, M. F. M.-Tovar, R. Farooq, R. Dongre, and S. Riaz, IntechOpen 145–160. (2019).
11. Wang, W. et al. Biodetection and bioremediation of copper ions in environmental water samples using a temperature-controlled, dual-functional Escherichia coli cell. *Appl. Microbiol. Biotechnol.* **103**, 6797–6807 (2019).
12. Cséfalvay, E., Pauer, V. & Mizsey, P. Recovery of copper from process waters by nanofiltration and reverse osmosis. *Desalination* **240**, 132–142 (2009).
13. Schlesinger, M. E., Sole, K. C. & Davenport, W. G. and G. R. F. Alvear Flores, Extractive Metallurgy of Copper, 6th ed., Elsevier (2021).
14. Tzaneva, B., Petrova, T., Hristov, J. & Fachikov, L. Electrochemical investigation of cementation process. *Bulg. Chem. Commun.* **48**, 91–95 (2016).
15. Popov, K. I., Djokić, S. S. & Grgur, B. N. *Fundamental Aspects of Electrometallurgy* (Kluwer Academic, 2002).
16. Demirkıran, N., Ekmekyapar, A., Künkül, A. & Baysar, A. A kinetic study of copper cementation with zinc in aqueous solutions. *Int. J. Min. Process.* **82**, 80–85 (2007).
17. Shahrivar, E., Karamoozian, M. & Gharabaghi, M. Modeling and optimization of oxide copper cementation kinetics. *Sn Appl. Sci.* **2**, 469 (2020).
18. Ahmed, I. M., El-Nadi, Y. A. & Daoud, J. A. Cementation of copper from spent copper-pickle sulfate solution by zinc Ash. *Hydrometallurgy* **110**, 62–66 (2011).
19. Hsu, Y. J., Kim, M. J. & Tran, T. Electrochemical study on copper cementation from cyanide liquors using zinc. *Electrochim. Acta*. **44**, 1617–1625 (1999).
20. Mubarak, A. A. Removal of copper from dilute solutions by cementation on zinc in baffled batch-agitated vessels. *Chem. Biochem. Eng. Q.* **20**, 79–83 (2006).
21. Mubarak, A. A., El-Shazly, A. H. & Konsowa, A. H. Recovery of copper from industrial waste solution by cementation on reciprocating horizontal perforated zinc disc. *Desalination* **167**, 127–133 (2004).
22. Nosier, S. A., Alhamed, Y. A. & Alturaif, H. A. Enhancement of copper cementation using ceramic suspended solids under single phase flow. *Sep. Purif. Technol.* **52**, 454–460 (2007).
23. Konsowa, A. H. Intensification of the rate of heavy metal removal from wastewater by cementation in a jet reactor. *Desalination* **254**, 29–34 (2010).
24. Amin, N. K. & El-Ashtokhy, E. S. Z. Kinetic study of copper cementation onto zinc using a rotating packed bed cylindrical reactor. *Can. J. Chem. Eng.* **89**, 609–616 (2011).
25. El-Sayed, E. M. M., Zewail, T. M. M. & Zaatout, A. A. Production of copper powder from synthetic wastewaters by cementation on a longitudinal finned rotating zinc cylinder. *Desalin. Water Treat.* **57**, 19959–19964 (2015).

26. El-Shazly, A. H., Nassr, A. M., Mubarak, A. A. & Zaatout, A. A. Effect of operating conditions on the Cu^{2+} removal from wastewater by cementation on a fixed bed of zinc cylinders, desalin. *Water Treat.* **57**, 22835–22841 (2016).
27. Ibrahim, B. S. et al. Cementation of copper on zinc in agitated vessels equipped with perforated baffles as turbulence promoters. *Min. Metall. Explor.* **38**, 1203–1213 (2021).
28. Elzahaby, M. H., Nosier, S. A., Sedahmed, G. H., Fathalla, A. S. & Abdel-Aziz, M. H. El-Gayar, cementation of copper on zinc in an unsubmerged jet reactor. *Cana Metall. Q.* **62**, 311–321 (2023).
29. Cussler, E. L. *Diffusion: Mass Transfer in Fluid Systems* (Cambridge University Press, 2009).
30. Plawsky, J. L. *Transport Phenomena Fundamentals* 4th edn (CRC, 2020).
31. Ahmed, M. S. et al. Abdel-Aziz, enhancement of heavy metals recovery from aqueous solutions by cementation on a rotating cylinder using a stationary wiper. *J. Ind. Eng. Chem.* **97**, 460–465 (2021).
32. Farooque, M. & Fahidy, T. Z. The anodic oxidation of methanol via continous electrode reactivation. *Electrochim. Acta*. **24**, 547–533 (1979).
33. Takahashi, T., Ismail, M. I. & Fahidy, T. Z. Metal recovery in a pilot-scale rotating cylindrical wiper-blade electrode system. *Electrochim. Acta*. **26**, 1727–1735 (1981).
34. Findlay, A. & Kitchner, J. Practical physical chemistry, Longman, (London, 1965).
35. Lobo, V. M. M. Mutual diffusion coefficient in aqueous electrolyte solutions. *Pure Appl. Chem.* **65**, 2613–2640 (1993).
36. Ascanio, G., Castro, B. & Galindo, E. Measurement of power consumption in stirred vessels-A review. *Chem. Eng. Res. Des.* **82**, 1282–1290 (2004).
37. Walsh, F. *A First Course in Electrochemical Engineering* (The Electrochemical Consultancy, 1993).
38. Fogler, H. S. Elements of chemical reaction engineering, Prentice Hall PTR (2006).
39. McCabe, W. L. & Smith, J. C. *And P. Harriot Unit Operations of Chemical Engineering* 7th edn (McGraw Hill Inc., 2004).
40. El–Naggar, M. A. et al. Extraction of copper from liquid effluents by cementation in agitated vessels equipped with expanded aluminum cylindrical sheets. *J. Sustain. Metall.* **8** 1318–1329. (2022).
41. Alemany, C., Aurousseau, M., Lapicque, F. & Ozil, P. Cementation and corrosion at a RDE: changes in flow and transfer phenomena induced by surface roughness. *J. Appl. Electrochem.* **32**, 1269–1278 (2002).
42. Ekmekyapar, A., Tanaydin, M. & Demirkiran, N. Investigation of copper cementation kinetics by rotating aluminum disc from the leach solutions containing copper ions. *Physicochem Probl. Min. Process.* **48**, 355–367 (2012).
43. Griskey, R. G. *Transport phenomena and unit operations: A combined approach* (John Wiley & Sons, Inc., 2002).
44. Lee, E. C., Lawson, F. & Han, K. N. Effect of precipitant surface roughness on cementation kinetics. *Hydrometallurgy* **3**, 7–21 (1978).
45. Nadebaum, P. R. & Fahidy, T. Z. The rate of mass transfer at a rotating cylindrical electrode with wiper blades. *Can. J. Chem. Eng.* **53**, 259–267 (1975).
46. Miyashita, H. & Hoffman, T. W. Local heat transfer coefficients in scraped-film heat exchanger. *J. Chem. Eng. Jpn.* **11**, 444–450 (1978).

Author contributions

Author Contributions StatementA. S. Fathalla: Methodology, Investigation, Writing - Review & Editing, Formal analysis, Validation.E.-S. Z. El-Ashtoukhy: Methodology, Investigation, Writing - Review & Editing, Formal analysis, Validation.M. H. Abdel-Aziz: Methodology, Investigation, Writing - Review & Editing, Formal analysis, Validation.G. H. Sedahmed: Conceptualization, Writing - Review & Editing, Formal analysis, Supervision.M. A. El-Naggar: Methodology, Investigation, Writing - Review & Editing, Formal analysis, Validation.

Declarations

Competing interests

The authors declare no competing interests.

Additional information

Correspondence and requests for materials should be addressed to M.H.A.-A.

Reprints and permissions information is available at www.nature.com/reprints.

Publisher's note Springer Nature remains neutral with regard to jurisdictional claims in published maps and institutional affiliations.